OncoTargets and Therapy

Dovepress
Taylor & Francis Group

Open Access Full Text Article

ORIGINAL RESEARCH

SNRPE is Associated with ERK/mTOR Signaling Activation and Reduced Autophagy to Promote Lung Adenocarcinoma Cell Proliferation

Jun Yang[1,2], Wenchao Dai[1,2], Bi Ren[2], Hang Chen[1,2], Xin Dang[1,2], Li Jiang[1]

[1]Department of Respiratory and Critical Care Medicine, The Affiliated Hospital of North Sichuan Medical College, Nanchong, Sichuan, People's Republic of China; [2]Department of Clinical Medicine, North Sichuan Medical College, Nanchong, Sichuan, People's Republic of China

Correspondence: Li Jiang, Department of Respiratory and Critical Care Medicine, The Affiliated Hospital of North Sichuan Medical College, Nanchong, Sichuan, People's Republic of China, Email lanqilily@163.com

Objective: To explore the effect of small nuclear ribonucleoprotein E (SNRPE) on proliferation and autophagy in lung adenocarcinoma (LUAD).

Methods: SNRPE expression was measured in LUAD and para-cancerous tissues by immunohistochemical detection and in LUAD cell-lines by real-time fluorescence quantitative PCR (RT-qPCR) and Western blotting. Cell proliferation was evaluated by cell counting kit (CCK-8) and colony formation, cell cycle progression and apoptosis were assessed by flow cytometry. Extracellular signal-regulated kinase (ERK)/Mammalian target of rapamycin (mTOR) signaling and autophagy proteins, Microtubule-associated protein 1 light chain 3B (LC3B), Sequestosome-1 (P62) and Beclin1 were measured by Western blotting. The impact of SNRPE expression on tumor growth in vivo was assessed by an animal model of LUAD.

Results: LUAD tissues showed high SNRPE expression and expression correlated with T stage. SNRPE knockdown in LUAD cells decreased proliferation, induced autophagy, trapped cells in G1 phase and inhibited the activation of ERK/mTOR signaling. Xenograft tumors with SNRPE knockdown showed reduced growth rate.

Conclusion: SNRPE was expressed at high levels in LUAD cancer tissues. SNRPE knockdown inhibited LUAD cell proliferation and stimulated autophagy in vivo and in vitro. SNRPE may target the ERK/mTOR signaling pathway. These findings may expose a novel target for LUAD treatment. In this study, limitations include the relatively small clinical sample size, lack of autophagy flux assays, and absence of mechanistic rescue experiments, which warrant further studies.

Plain Language Summary: Lung adenocarcinoma is a common type of lung cancer that often grows quickly and is difficult to treat. In this study, we focused on a protein called SNRPE, which is found in high amounts in lung cancer tissues. Our experiments in cells and mice showed that lowering SNRPE levels slowed cancer cell growth and increased a cell-cleaning process called autophagy, likely linked to reduced activity in the ERK/mTOR signaling pathway. These findings, based on laboratory models, suggest SNRPE may contribute to lung cancer growth, but more research is needed to confirm these effects and explore SNRPE as a potential treatment target.

Keywords: lung adenocarcinoma, small nuclear ribonucleoprotein E, ERK/mTOR, LC3, P62 autophagy

Introduction

Lung cancer is the second most prevalent neoplasm with an annual global incidence of 11.6% and the foremost contributor to cancer-related mortality, accounting for 18.4% total cancer deaths.[1,2] Non-small cell lung cancer (NSCLC) represents 80–85% of lung cancer cases and has an unfavorable prognosis with 5-year overall survival of 5–10%, a value that has not shown much recent improvement.[3–5] NSCLC may be classified into lung adenocarcinoma (LUAD), accounting for 55% cases, and lung squamous carcinoma (LUSC).[6,7] Although a variety of therapies, including

Received: 12 May 2025
Accepted: 7 November 2025
Published: 15 November 2025

chemotherapy and surgical resection, can reduce the mortality rate of LUAD, a number of challenges remain, including the late detection of about 75% of LUAD patients, a high rate of recurrence, and a poor prognosis.[7] The disease is a particular problem in China with economic, population health and social impacts.[8] Therefore, there is an urgent need to find new therapeutic targets for the treatment of LUAD.

The mitogen-activated protein kinase (MAPK) signaling pathway is known to be involved in neoplastic transformation and disease progression.[1] Extracellular signal-regulated kinase (ERK) is involved in cytokine regulation of mitosis, phenotypic specification and apoptosis resistance with actions on tumor cell migration and invasion.[9] ERK activation has been linked to malignant pathogenesis.[10,11] Mammalian target of rapamycin (mTOR) is a master regulator of anabolic processes, including synthesis of nucleic acids, proteins, lipids and ribosomes, and suppresses catabolic activities, such as lysosome formation and autophagic flux.[12] The involvement of ERK/mTOR signaling in cell tumor cell proliferation, migration and invasion has been highlighted by observations of the impact on autophagy and drug resistance.[13–15]

Small nuclear ribonucleoproteins (snRNP) have many functions, one of which is to encode structural components of the spliceosome that is responsible for processing intron removal from precursor mRNA.[16] Five snRNPs plus additional non-snRNP splicing proteins mediate splicing and disorder of this process has been linked to cancer, genetic diseases and neurodegenerative disorders.[17,18] The snRNP, small nuclear ribonucleoprotein polypeptide E (SNRPE), has been suggested to influence malignancies with hyper-differentiation features, such as hepatocellular carcinoma, and increased SNRPE protein observed in prostate and bladder cancers.[19,20]

While studies have implicated SNRPE in LUAD through its role in spliceosome function and proliferation,[21–23] its specific effects on ERK/mTOR signaling and autophagy in LUAD remain underexplored. Given the emerging evidence of SNRPE's role in cancers, we hypothesized that SNRPE promotes LUAD progression by enhancing proliferation and suppressing autophagy through the ERK/mTOR signaling pathway. The primary objective of this study was to evaluate SNRPE expression in LUAD tissues and cell lines, assess its impact on proliferation and autophagy, and explore its mechanistic link to ERK/mTOR signaling, with the aim of identifying a potential therapeutic target.

Materials and Methods

Bioinformatics Analysis

Bioinformatic analysis of SNRPE expression was conducted in cancer tissue samples from The Cancer Genome Atlas (TCGA) and the genotype tissue expression (GTEx) project via the Gene Expression Profiling Interactive Analysis (GEPIA) platform (http://gepia.cancer-pku.cn) and the University of Alabama at Birmingham Cancer Analysis Portal (UALCAN) database (http://ualcan.path.uab.edu). SNRPE expression was assessed in LUAD and paraneoplastic tissues and correlated with patient prognosis and survival.

Patient Data and Tissue Specimens

Tumor and paired para-cancerous tissues were collected from 40 primary LUAD patients, 23 male and 17 female, of median age 63.5 years (range: 45–82 years) who underwent surgical resection at the Affiliated Hospital of North Sichuan Medical College in Nanchong, China, between January 2019 and December 2021. 17 patients had a history of smoking and 23 did not. No patient had received preoperative chemotherapy or radiotherapy. All experiments were conducted in accordance with the Declaration of Helsinki (amended 2024) and all patients gave written informed consent for treatment of samples and publication of data. Ethical approval was granted by the Medical Ethics Committee of the Affiliated Hospital of North Sichuan Medical College (Ethical Approval No. 2024ER552-1).

Immunohistochemistry

Paraffin-embedded sections of cancerous and para-cancerous tissues were deparaffinized, hydrated, antigenically repaired, peroxidase inhibitor added and samples blocked with goat serum. Primary anti-SNRPE antibody (diluted 1:150; Affinity, 1:150) was added dropwise and samples incubated overnight at 4 °C. Biotin-tagged secondary antibody (Servicebio, 1:100) was added for 30 minutes, DAB substrate added for 3 minutes and hematoxylin restaining performed for 3 minutes. Slides were washed with water to develop the blue color, dehydration with ethanol gradient performed and

xylene added with neutral gum to seal the film. Immunohistochemical microscopic scoring was performed by two pathologists with over 10 years' work experience under double-blind conditions. Values for chromogenic signal intensity and percentage positive cells were multiplied to give the immunoreactivity score (IRS). Histochemical intensity was graded as 0 (undetectable signal), 1 (subtle light-yellow reactivity), 2 (discernible brownish-yellow pigmentation) and 3 (pronounced tan deposition). Percentage positive cells value was categorized into four tiers: minimal reactivity (≤ 25% immunoreactive cells), focal distribution (26–50% stained populations), multifocal expression (51–75% antigen-positive elements) and diffuse manifestation (> 75% immunolabeled constituents).

Cell Culture

Two human LUAD cell lines, H1299, a NSCLC cell isolated from the lymph node which has epithelial properties, and A549, isolated from a primary adenocarcinoma tumor, were selected for study and purchased from Wuhan Pricella Life Sciences Co., Ltd. H1299 cells were grown in RPMI1640 and A549 in F-12K medium both with 10% fetal bovine serum and antibiotics (all media from Wuhan Procell Biotechnology Co., Ltd., Hubei, China) in 5% CO_2 at 37 °C.

SNRPE Knockdown

Lentiviral vectors for SNRPE knockdown, LV-SNRPE-RNAi (shSNRPE), or control, LV-NC-RNAi (shNC), with GFP tag and puromycin resistance genes were synthesized by GENE, China. The shSNRPE sequence was 5′-GATGAGTATATATGAACCTTGTA-3′ and the NC sequence was 5′-TTCTCCGAACGTGTCACGT-3′. H1299 and A549 cells were grown to 40–50% confluence in six-well plates, transfected with vectors and incubated with puromycin to select for shSNRPE uptake. Transfected cells were grown with 2 μg/mL puromycin for over 7–10 days for the selection.

Real-Time Fluorescence Quantitative PCR (RT-PCR)

RNA was isolated with TRIzol (Epizyme, Shanghai, China) reagent, according to the manufacturer's instructions, and first-strand cDNA synthesis performed to eliminate genomic DNA contamination. qPCR was performed with ChamQ SYBR qPCR Master Mix (Vazyme, Nanjing, China) on a StepOnePlus™ Real-Time PCR System. SNRPE expression was normalized to the expression of the housekeeping gene, GAPDH. Primer sequences (Sangon Biotech) were GAPDH Forward: 5′-GGAGTCCACTGGCGTCTTCA-3′, Reverse: 5′-GTCATGAGTCCTTCCACGATACC-3′ and SNRPE Forward: 5′-TGAATATATGCGGATAGAA-GGCTGT-3′, Reverse: 5′-TGGAGACACTTTGTAGCAGAGT-3′. Fold change in expression was calculated by the $2^{-\Delta\Delta CT}$ method.

Western Blotting

Cells were lysed with RIPA buffer (Epizyme, Shanghai, China) containing dual enzyme inhibitors and total protein measured by BCA Protein Assay Kit (Epizyme, Shanghai, China), according to the manufacturer's instructions. Equal quantities protein/well were separated by SDS-PAGE, transferred to PVDF membranes and sealed with protein-free rapid closure solution. Membranes were incubated with primary antibodies: anti-SNRPE antibody (Affinity Biosciences, Changzhou, China; 1:1000), anti-ERK & p-ERK antibodies (Epizyme, Shanghai, China; 1:1500); anti-mTOR & p-mTOR antibodies (Epizyme, Shanghai, China; 1:3000); anti-LC3B antibody (Epizyme, Shanghai, China; 1:3000); anti-P62 antibody (Epizyme, Shanghai, China; 1:2000); anti-Beclin1 antibody (Epizyme, Shanghai, China; 1:3000); anti-GAPDH antibody (FineTest, Wuhan, China; 1:5000); anti-Tubulin antibody (FineTest, Wuhan, China; 1:5000) overnight at 4 °C (16–18 hr), followed by incubation for 1 hr at room temperature with goat anti-rabbit secondary IgG (Epizyme, Shanghai, China; 1:5000) and visualization with ECL kit (Epizyme, Shanghai, China). Quantitative densitometry was carried out with ImageJ software.

Cell Proliferation Assay

Cells were inoculated into 96-well plates at a density of 5×10^4 cells/mL, cultured under standard conditions and viability assessed at 0 h, 24 h, 48 h and 72 h by CCK-8 kit (APE-xBIO, USA), following the manufacturer's protocol. In brief,

a 1:10 ratio of CCK-8 solution was added to wells for 2 h incubation before the 450 nm absorbance values were read by microplate reader.

Colony Formation Assay

Cells were inoculated into 6-well plates at a density of 1000 cells per well and cultured for 10 to 14 days at 37 °C with 5% CO_2 until colonies were visible to the unaided eye. Cells were washed 3 times with PBS, fixed with 4% paraformaldehyde for 20 min and stained with 0.1% crystal violet for 20 min for microscopic inspection.

Cell Cycle Assay

Cells were harvested, washed twice with pre-chilled PBS, fixed in 70% ethanol at 4 °C overnight and 70% ethanol added at 4 °C for 1h. Cells were stained with RNAase and propidium iodide (KeyGEN BioTECH) at room temperature for 1h in the dark, following the manufacturer's guidelines. A flow cytometer was used for cell cycle analysis.

Apoptosis Assay

Cells were harvested, washed with chilled PBS, resuspended in 1 x Binding Buffer and incubated with Annexin V - APC/PI working solution at room temperature for 10 minutes in the dark. Apoptotic cells were assessed by flow cytometry. The Annexin V-APC/PI apoptosis detection kit was purchased from KeyGEN BioTECH, Nanjing, China.

Animal Experiments

Male BALB/c-nu nude mice (4 weeks, 20–25 g weight, n = 10 Beijing Spectrum Biotechnology Co., Ltd.) were housed under SPF conditions with a 12 h light/12 h dark cycle and access to food and water ad libitum. Mice were inoculated in the right dorsal subcutaneous flank with 3×10^6 cells/pc A549 cells transfected with shSNRPE (n = 5) or A549 cells transfected with shNC (n = 5).

Mice were weighed weekly; tumor growth monitored with digital calipers and mice sacrificed after 4 weeks. All animal experiments were performed in compliance with the ethical guidelines of the Institutional Animal Care and Use Committee at North Sichuan Medical College (Nanchong, China; approval number: 2025004). Sample size for animal experiments (n=5 per group) was based on prior studies but may be underpowered; future studies should include larger sample sizes to ensure statistical robustness.

Statistical Analysis

Statistical analyses were performed with SPSS 26.0 and GraphPad Prism 10.0. Data are presented as mean ± standard deviations of at least 3 replicates. Group comparisons were made by *t*-test for two groups and one-way ANOVA for multiple groups. Shapiro–Wilk test was used to examine the normality of data distributions prior to applying t-tests or ANOVA. No significant deviation from normality was observed. For multiple comparisons, ANOVA was followed by Tukey's post hoc test. Associations of SNRPE expression and clinicopathological parameters were assessed by chi-square test (χ^2) and *P*-value < 0.05 considered to indicate statistical significance.

Results

SNRPE Expression was Elevated in a Range of Tumors

SNRPE expression was assessed in a range of tumor types compared with normal tissues from the GEPIA database and results validated using the UALCAN database. SNRPE expression was higher in bladder migratory cell carcinoma, breast cancer, cervical squamous cell carcinoma, LUAD, lung squamous carcinoma, colon cancer, esophageal cancer, glioblastoma and gastric carcinoma than in non-tumor tissues (Figure 1A and B).

SNRPE Expression Correlated with LUAD Patient Prognosis

In this study, the expression data of SNRPE in The Cancer Genome Atlas (TCGA) dataset and GTEx database were obtained from the GEPIA platform for differential expression analysis and prognostic survival analysis, and the results

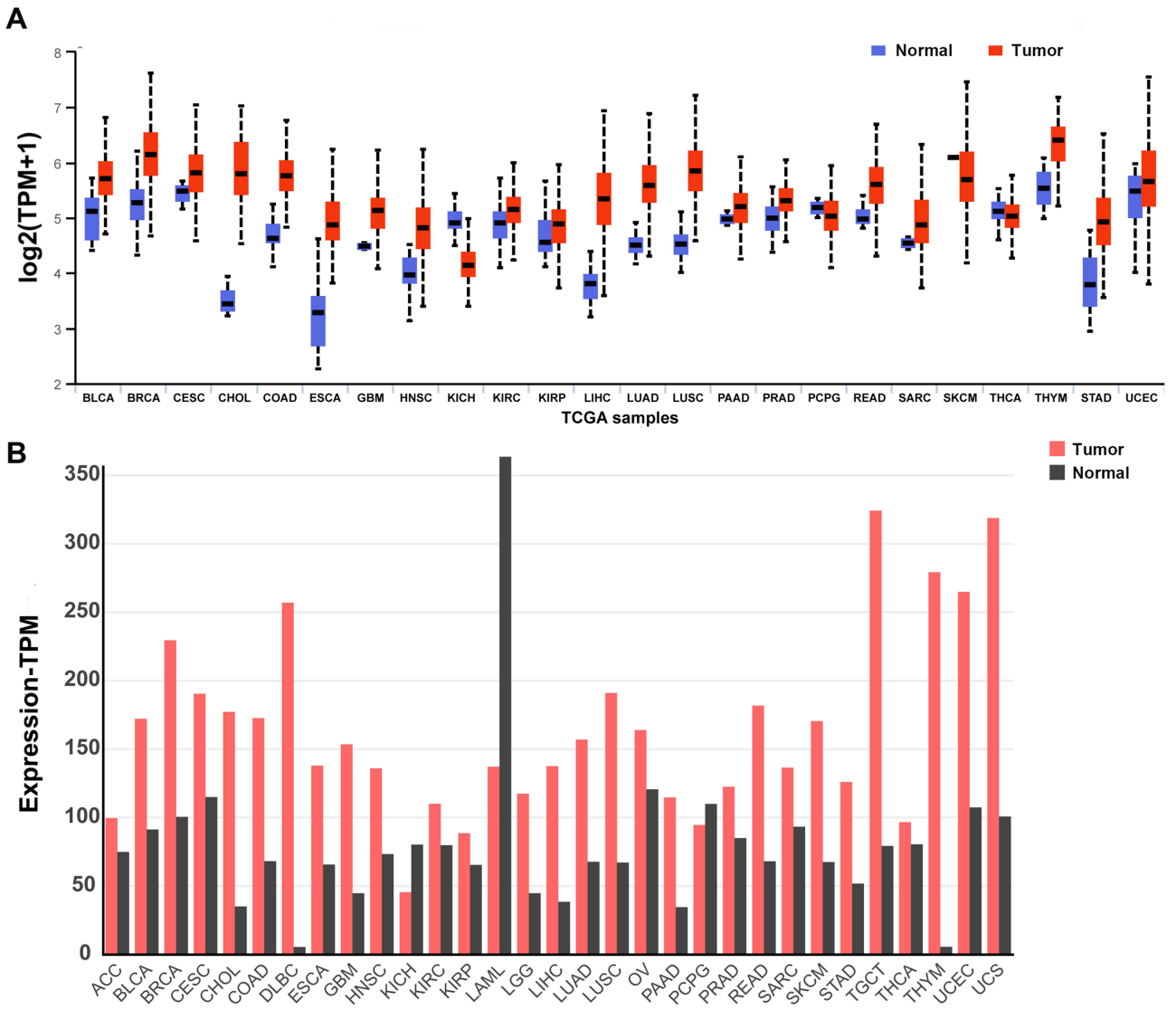

Figure 1 SNRPE expression in a range of cancer tissue samples from TCGA. (**A**) SNRPE levels in cancerous and non-cancerous tissues; (**B**) SNRPE expression in paired cancerous and non-cancerous tissues.

were validated using the UALCAN database. The results showed that the expression level of SNRPE in lung adenocarcinoma tissues was higher than that in normal tissues (Figure 2A, $P < 0.05$). The results of the analysis in the UALCAN database were in agreement with those of the GEPIA platform (Figure 2B–D, $P < 0.05$). The prognosis of patients in the group with low SNRPE expression was better than that in the group with high SNRPE expression (Figure 2C, $P < 0.05$). The above results indicated that the higher SNRPE expression suggested a poor prognosis.

SNRPE Expression was Associated with Clinicopathological LUAD Characteristics

Assessment of SNRPE expression in cancerous and adjacent non-cancerous tissues from 40 LUAD patients indicated overexpression in malignant samples (Figure S1A and B). SNRPE expression in cancerous and adjacent non-cancerous tissues from 40 LUAD patients revealed significantly higher SNRPE expression in malignant samples compared to para-cancerous tissues (Figure S1A and B, $P < 0.01$). Using the median IRS score (IRS = 4) as a cutoff, 24 cases (60%) were categorized as low expression (IRS ≤ 4), and 16 cases (40%) as high expression (IRS > 4), with high expression significantly correlated with tumor T-stage (Table 1). No statistically significant associations were found for age, gender, history of smoking or histological classification. These findings highlight the association of high SNRPE expression with malignancy and raise

https://doi.org/10.2147/OTT.S539944

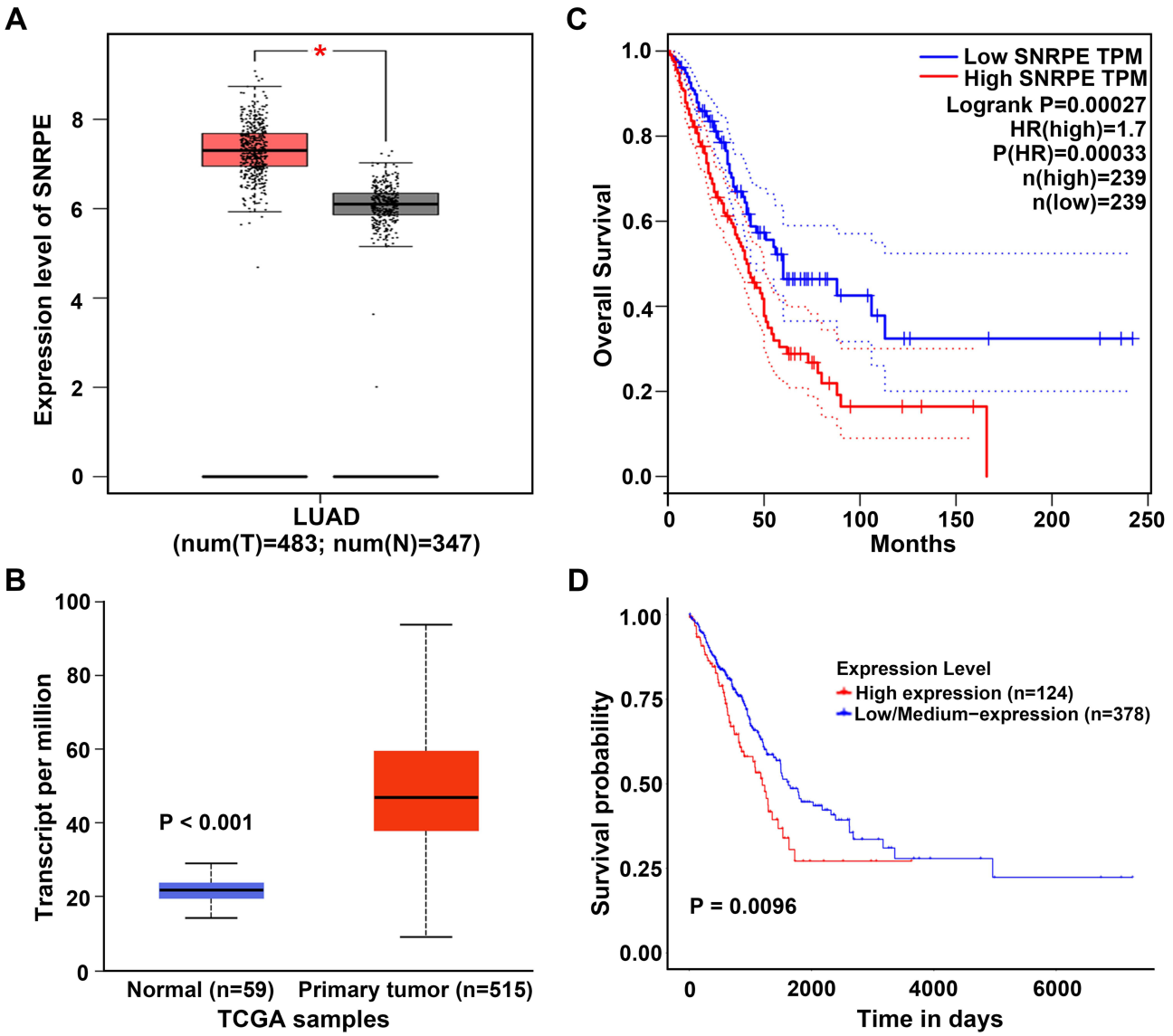

Figure 2 Bioinformatics analysis of SNRPE expression in LUAD and impact on patient survival. (**A** and **B**) SNRPE expression in LUAD and non-cancerous tissues from the UALCAN database. Expression differences between normal and tumor tissues were also highly significant ($P < 1 \times 10^{-12}$); (**C**) Patients from the UALCAN database were divided into low and high expressing groups based on median SNRPE expression and OS assessed; (**D**) Survival analysis of low (blue) and high (red) SNRPE expressing LUAD patients. *$P < 0.05$, $P < 0.01$ indicates significant differences.

the possibility that SNRPE expression level may be linked to tumor progression. These results are consistent with previous studies which have linked SNRPE expression to cancer pathogenesis and extend such observations to include LUAD.

SNRPE Knockdown Inhibited H1299 and A549 Cell Proliferation

Transfection of H1299 and A549 cells with shSNRPE resulted in successful reduction of SNRPE mRNA expression (Figure S2A) and SNRPE protein (Figure S2B). Lentiviral transfection with shSNRPE was used to knock down the level of SNRPE in LUAD cells and SNRPE knockdown inhibited cell proliferation (Figure 3A and B) and colony formation (Figure 3C–F).

SNRPE Knockdown Caused Cell Cycle Arrest but Did Not Induce Apoptosis

Flow cytometry analysis of SNRPE knockdown A549 and H1299 cells showed prolongation of G1 phase in both cell types (Figure S3A–D). No significant increase in numbers of Annexin V-positive cells was found indicating that SNRPE knockdown did not stimulate apoptosis (Figure S3E and F). Thus, knockdown of SNRPE appears to cause cell cycle

Table 1 SNRPE Expression and Clinicopathological Characteristics of LUAD Patients

Characteristics	Cases	Low Expression of SNRPE	High Expression of SNRPE	χ^2	*P*-value
Age					
< 60	14	8	6	0.073	0.786
≥ 60	26	16	10		
Sex					
Male	23	11	12	3.342	0.0675
Female	17	13	4		
History of smoking					
Yes	17	9	8	0.613	0.4334
No	23	15	8		
Clinical stages					
I	26	17	9	0.897	0.638
II	6	3	3		
III+IV	8	4	4		
T stage					
T1+T2	33	23	10	7.388	0.006
T3+T4	7	1	6		
N stage					
N0	31	19	12	0.095	0.757
N1+N2+N3	9	5	4		
M stage					
M0	39	24	15	/	/
M1	1	0	1		

arrest in both LUAD cell types, suggesting that high SNRPE levels in malignant cells may stimulate proliferation by promoting cell cycle progression.

SNRPE Knockdown May Stimulate Autophagy in A549 and H1299 Cells

SNRPE knockdown increased Microtubule-associated protein 1 light chain 3 (LC3) levels by 54% and Beclin1 levels by 58% while reducing Sequestosome-1 (P62) expression by 50% in A549 cells (Figure 4A and B). Similarly, LC3 was increased by 40%, Beclin1 by 50% and P62 was decreased by 50% in SNRPE knockdown H1299 cells relative to controls (Figure 4C and D). These changes indicate the stimulation of autophagy in A549 and H1299 cells with SNRPE knockdown, suggesting that high SNRPE expression in malignant cells may act as a suppressor of autophagy.

Expression of ERK/mTOR Signaling Proteins in SNRPE Knockdown A549 and H1299 Cells

SNRPE knockdown reduced levels of the phosphorylated proteins, p-ERK and p-mTOR, which are considered to indicate the activated state of the pathway but did not change quantities of total ERK and mTOR. Levels of p-ERK were reduced by 70% in A549 SNRPE knockdown cells and by 60% in H1299 SNRPE knockdown cells relative to controls (Figure 5A and B). Levels of p-mTOR were reduced by 58% in A549 SNRPE knockdown and by 70% in H1299 SNRPE knockdown cells (Figure 5C and D). Knockdown of SNRPE appears to reduce the activation state of ERK/mTOR signaling, suggesting that high levels of SNRPE in malignant cells may result in over-activation of this signaling pathway. This would be consistent with the observations from bioinformatic analysis and from patient samples that high levels of SNRPE expression are correlated with malignancy.

SNRPE Promoted Tumorigenesis in vivo

Mouse xenograft models of human LUAD tumors were created by inoculating animals with A549 cells transfected with either shSNRPE or shNC. SNRPE knockdown tumors grew to smaller sizes and volume was reduced 6-fold after 28

https://doi.org/10.2147/OTT.S539944

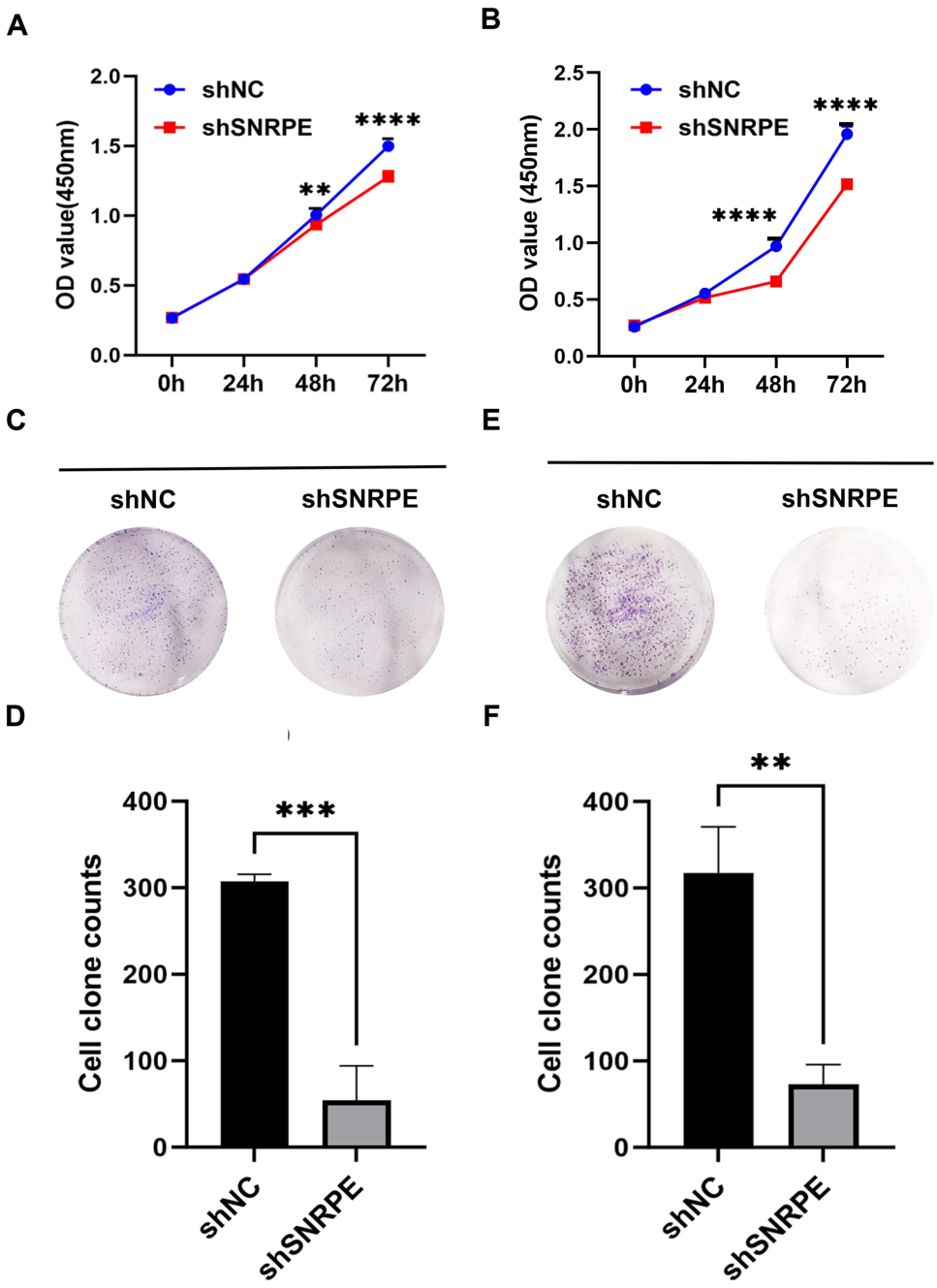

Figure 3 Cell proliferation and colony formation in SNRPE knockdown A549 and H1299 cells. (**A**) Measurements of proliferation in SNRPE-knockdown A549 cells by CCK-8 assay; (**B**) Measurements of proliferation in SNRPE-knockdown H1299 cells by CCK-8 assay; (**C**) Representative images of colony formation by SNRPE knockdown A549 cells; (**D**) Quantitative analysis of colony formation by SNRPE knockdown A549 cells; (**E**) Representative images of colony formation by SNRPE knockdown H1299 cells; (**F**) Quantitative analysis of colony formation by SNRPE knockdown H1299 cells. $^{**}P < 0.01$, $^{***}P < 0.001$, $^{****}P < 0.0001$.

days, relative to SNRPE-expressing tumors (Figure 6). IHC staining to assess expression of the cell proliferation marker, ki67, showed 20% lower levels in SNRPE knockdown tumors (Figure S4A–D). The finding that lower levels of proliferating cells are present in tumors with SNRPE knockdown suggests that the high expression of SNRPE seen in most tumors in vivo contributes to high rates of tumor growth.

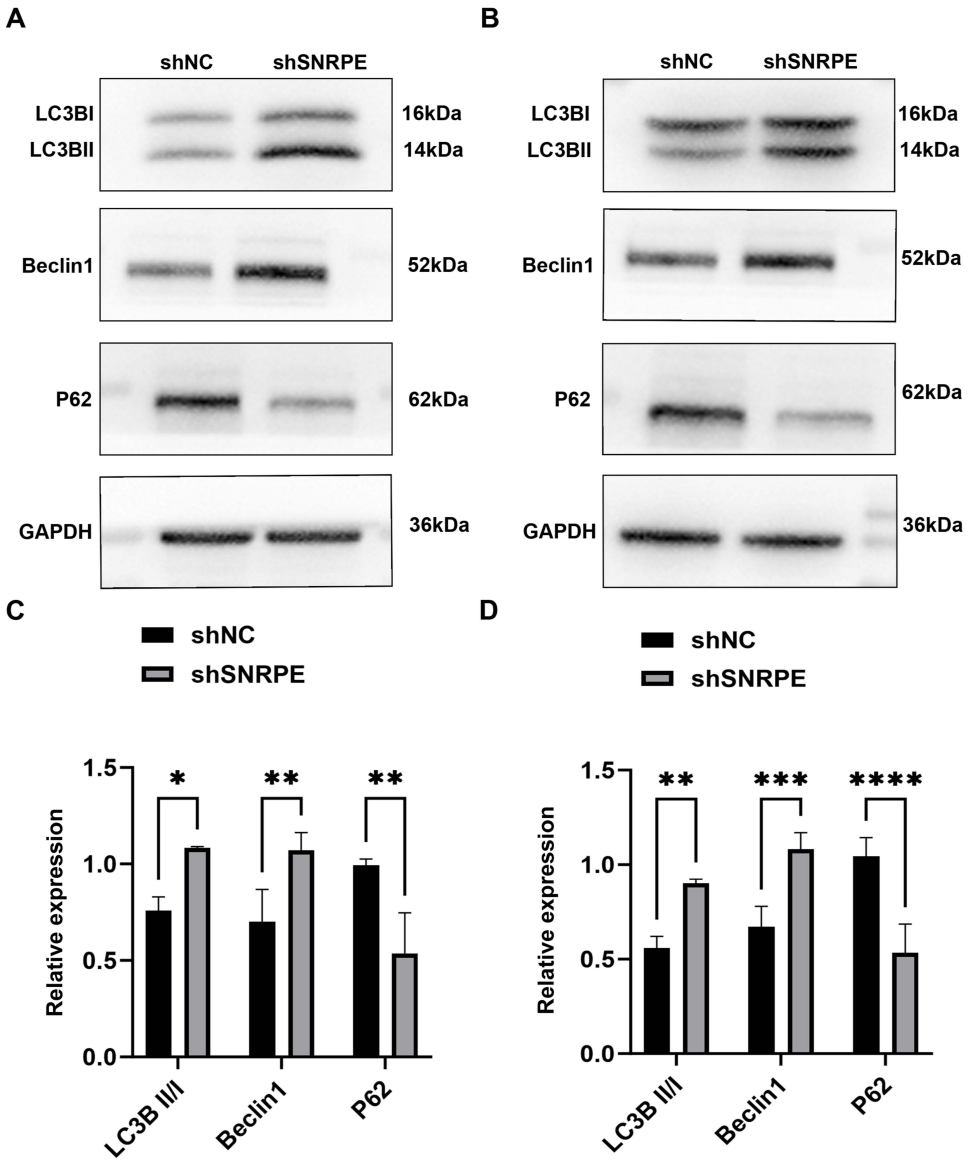

Figure 4 Levels of LC3, Beclin1 and P62 proteins in SNRPE knockdown A549 and H1299 cells. (**A**) Western blotting images showing expression of LC3, Beclin1 and P62 in A549 cells transfected with shSNRPE or shNC. GAPDH was included as a loading control; (**B**) Western blotting images showing expression of LC3, Beclin1 and P62 in H1299 cells transfected with shSNRPE or shNC. GAPDH was included as a loading control; (**C**) Densitometric analysis of Western blots shown in (**A**). Quantities of proteins were normalized to GAPDH expression; (**D**) Densitometric analysis of Western blots shown in (**B**). Quantities of proteins were normalized to GAPDH expression. **P* < 0.05, ***P* < 0.01, ****P* < 0.001, *****P* < 0.0001.

Discussion

Prognosis remains poor for lung cancer patients and one factor influencing high mortality rates is early metastasis.[24] The current work indicates the contribution made by high expression of the small nuclear ribonucleoprotein, SNRPE, to aggressive and malignant behavior by LUAD cells in vitro and in vivo. SNRPE shows elevated expression in many cancer types, including LUAD, and activated proteins of the ERK/mTOR signaling pathway in the LUAD cells of the present work which may account for its stimulatory impact on tumor growth. SNRPE was also shown to change the expression of markers of autophagy. The present study increases the knowledge about molecular targets of SNRPE action and may contribute to the identification of therapeutic strategies.

There have been encouraging recent advances in anti-cancer therapies targeting specific molecules for treatment of breast carcinoma,[25] ovarian neoplasms[26] and NSCLC[27] and the current work may contribute to similar approaches for LUAD.[23] There have been many indications of disordered expression of small nuclear ribonucleoproteins (snRNPs) in

https://doi.org/10.2147/OTT.S539944

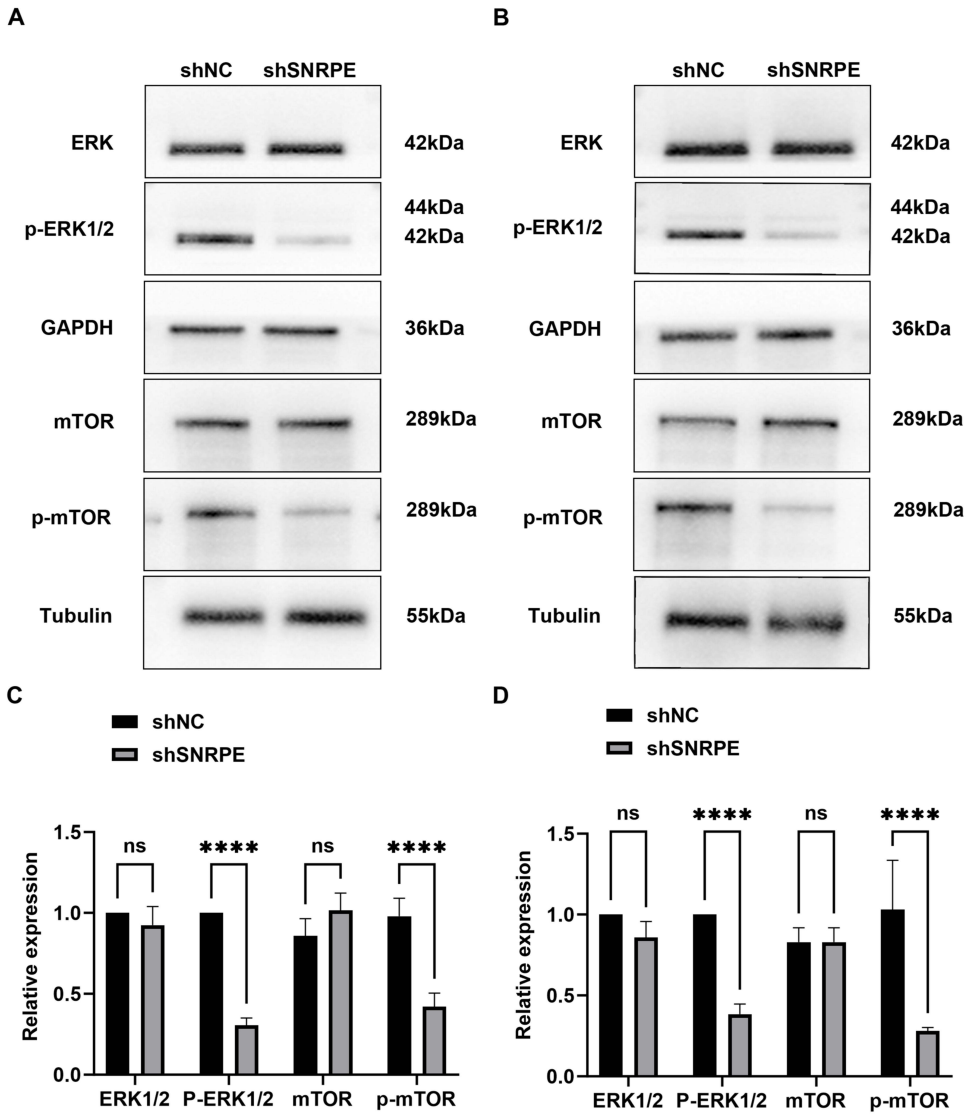

Figure 5 Expression of p-ERK and p-mTOR in A549 and H1299 cells with SNRPE knockdown. (**A**) Western blotting images showing expression of ERK, p-ERK, mTOR and p-mTOR in A549 cells transfected with shSNRPE and shNC. GAPDH and tubulin were included as loading controls; (**B**) Western blotting images showing expression of ERK, p-ERK, mTOR and p-mTOR in H1299 cells transfected with shSNRPE and shNC. GAPDH and tubulin were included as loading controls; (**C**) Densitometric analysis of data shown in (**A**). Values were normalized to GAPDH levels; (**D**) Densitometric analysis of data shown in (**B**). Values were normalized to GAPDH levels. ****$P < 0.0001$. **Abbreviation**: ns, not significant.

tumorigenesis, including in cervical carcinoma,[28] NSCLC,[29] glioblastoma,[30] breast cancer[31] and hepatocellular carcinoma.[32–34] Seven conserved SNRP genes, SNRPB, SNRPD1-3, SNRPE, SNRPF and SNRPG, are thought to encode components of the spliceosome which is responsible for processing of pre-mRNA to generate mature mRNA.[35] SNRPE proteins are core components of the spliceosome and the splicing process influences proliferation, programmed cell death and cellular motility, all of which are involved in tumorigenesis.[34] Indeed, snRNPs have been found to affect cervical cancer progression and suggested as potential therapeutic targets.[36] SNRPB acting through RAB26 has been implicated in NSCLC tumorigenesis and in combination with C-MYC to drive hepatocellular carcinoma cell proliferation. As a result, SNRPB has been defined as an oncogene.[29,37,38] SNRPE is known to be overexpressed in hepatocellular carcinoma and knockdown reduced the proliferation of HepG2 cells,[33] consistent with the findings of the current study for LUAD cells. In addition, SNRPE has been linked to prostate cancer tumorigenesis and shown to have potential as a therapeutic target[39] and microarray data analysis showed elevated SNRPE expression to be associated with adverse clinical outcomes, including reduced disease-free survival, in bladder cancer patients.[40,41]

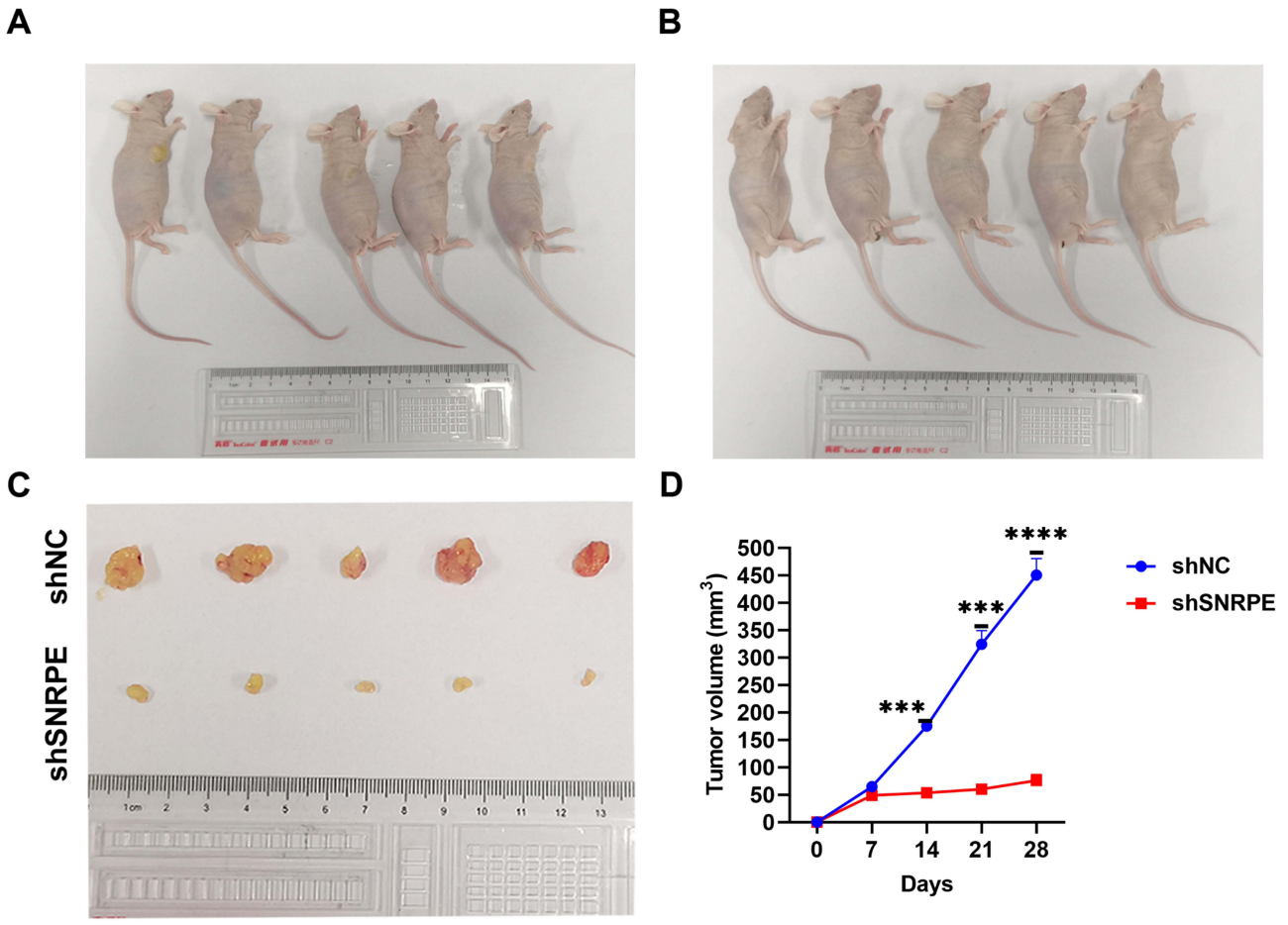

Figure 6 Growth of xenograft human tumors seeded from A549 LUAD cells with and without SNRPE knockdown in nude mice. (**A**) Tumor formation from A549 cells transfected with shNC; (**B**) Tumor formation from A549 cells transfected with shSNRPE; (**C**) Excised tumors from SNRPE knockdown and NC xenograft tumors; (**D**) Tumor volumes over time for xenograft tumors from SNRPE knockdown and NC A549 cells. ***$P < 0.001$, ****$P < 0.0001$.

Indeed, the role of SNRPE in differential splicing, demonstrated by ene profiling expression analysis and model prediction, has led to its identification as a high risk factor and prognostic in multiple myeloma and adrenocortical carcinoma.[42,43] SNRPE downregulation was found to reduce mTOR mRNA and protein levels and to induce autophagy in breast cancer[40] and these findings are consistent with the results of the present study which found that SNRPE knockdown reduced ERK/mTOR activation and increased expression of autophagy markers in LUAD cells. SNRPE and SNRPD1 promoted growth of lung, highly invasive breast and ovarian cancers by suppressing autophagy rather than apoptosis and it has been suggested that targeting of SNRPE or SNRPD1 splicing machinery may trigger mTOR blockade and autophagy.[44,45]

The autophagy protein, LC3, influences autophagosome membrane structure during maturation into autophagic lysosomes, making it an ideal marker for autophagy and expression of another autophagy protein, Beclin1, has been correlated with tumor aggressiveness, treatment resistance and clinical outcomes.[46,47] Beclin1 down-regulation was associated with malignant tumor progression and high expression with a favorable prognosis.[48,49] In addition, Beclin1-mediated autophagy has potential applications in tumor immunity and drug sensitivity.[48] P62 accumulation has been associated with defective autophagy and tumor progression and high expression linked to poor patient prognosis in ovarian cancer,[50] although autophagic activity can only be accurately estimated from P62 levels in combination with the LC3-II/LC3-I ratio.[51] P62 may also affect the sensitivity of breast cancer cells to chemotherapeutic agents, such as doxorubicin.[52] In Beclin1 overexpressing SW982 cells, autophagic activity was enhanced and LC3-II expression was elevated while P62 levels were significantly decreased.[53] The findings of the current study extend these previous

https://doi.org/10.2147/OTT.S539944

observations regarding the influence of autophagy on tumor cell growth. SNRPE was found to affect levels of LC3, Beclin1 and P62 and SNRPE knockdown stimulated the markers of autophagy activation. High expression of SNRPE recorded for many tumor types, including LUAD, may contribute to high rates of tumor growth by the inhibition of autophagy.

In the future, more in-depth research will be conducted on the upstream and downstream signaling pathways and other phenotypes of SNRPE, with the expectation of developing SNRPE inhibitors to reverse-validate the effects on LUAD, and elucidating the potential of SNRPE as a diagnostic, individualized treatment, and prognostic judgment of lung adenocarcinoma. However, there are still many deficiencies in this study, the first is that the amount of clinicopathological samples is small and the specimens are from recent years, the survival data are still insufficient to assess the survival prognosis, and the subsequent study will continue to improve and supplement; the second is that the evidence of SNRPE-mediated autophagy is insufficient, and the presence of autophagy can be assessed comprehensively by combining transmission electron microscopy (TEM) methods and acridine orange cell staining. Thirdly, the research on animal experiments is relatively weak, and we will continue to extract tissue mRNA and protein for the detection of relevant indexes, and if possible, we can carry out experiments on tumor xenograft model of patient origin to explore this gene. Future in vivo studies should also incorporate H1299-based xenografts to validate the consistency of SNRPE's effects across different LUAD cell lines. Additionally, while our findings suggest SNRPE as a potential candidate for therapeutic targeting in LUAD, the associative nature of the data and lack of causal experiments such as rescue studies, pathway inhibition need further validation. Future research should include SNRPE re-expression, pharmacologic inhibition of ERK/mTOR, and autophagy flux assays to establish mechanistic causality and therapeutic relevance.

Conclusion

SNRPE promoted proliferation of LUAD cells, A549 and H1299, in vitro and growth of a human xenograft LUAD tumor in a mouse model in vivo. SNRPE activated ERK/mTOR signaling and suppressed autophagy in A549 and H1299 cells. SNRPE is a potential biomarker for LUAD and may prove to be a potential target for anti-cancer therapy of LUAD.

Data Sharing Statement

The datasets generated and analyzed during the current study are available from the corresponding author on reasonable request.

Ethics Approval and Consent to Participate

The use of human tissue samples was approved by the Medical Ethics Committee of the Affiliated Hospital of North Sichuan Medical College (Approval No. 2024ER552-1), and written informed consent was obtained from all participants. All animal experiments were approved by the Animal Ethics Committee of North Sichuan Medical College (Approval No. 2025004).

Acknowledgments

We would like to thank the Science and Technology Innovation Center Laboratory of North Sichuan Medical College, the Institute of Hepatobiliary and Pancreatic Diseases of North Sichuan Medical College, and the Key Laboratory of Medical Imaging of North Sichuan Medical College for providing equipment and technical support.

Author Contributions

All authors have read and approved the final version of the manuscript. All authors made a significant contribution to the work reported, whether that is in the conception, study design, execution, acquisition of data, analysis and interpretation, or in all these areas; took part in drafting, revising or critically reviewing the article; gave final approval of the version to be published; have agreed on the journal to which the article has been submitted; and agree to be accountable for all aspects of the work.

Funding

This work was supported by the Nanchong Science and Technology Bureau (Grant No. 23JCYJPT0035), and The Affiliated Hospital of North Sichuan Medical College/Guang'an District People's Hospital Joint Development Research Program (Grant No. 2024LHFZ02).

Disclosure

The authors declare that they have no competing interests in this work.

References

1. Peng GQ, Song HC, Chen WY. Concomitant epidermal growth factor receptor mutation/c-ros oncogene 1 rearrangement in non-small cell lung cancer: a case report. *World J Clin Oncol*. 2024;15(7):945–952. doi:10.5306/wjco.v15.i7.945
2. Miao R, Xu Z, Han T, et al. Based on machine learning, CDC20 has been identified as a biomarker for postoperative recurrence and progression in stage I & II lung adenocarcinoma patients. *Front Oncol*. 2024;14:1351393. doi:10.3389/fonc.2024.1351393
3. Zhong T, Li Y, Jin M, et al. Downregulation of 4-HNE and FOXO4 collaboratively promotes NSCLC cell migration and tumor growth. *Cell Death Dis*. 2024;15(7):546. doi:10.1038/s41419-024-06948-4
4. Qu J, Mei Q, Liu L, et al. The progress and challenge of anti-PD-1/PD-L1 immunotherapy in treating non-small cell lung cancer. *Ther Adv Med Oncol*. 2021;13:1758835921992968. doi:10.1177/1758835921992968
5. Duma N, Santana-Davila R, Molina JR. Non-small cell lung cancer: epidemiology, screening, diagnosis, and treatment. *Mayo Clin Proc*. 2019;94(8):1623–1640. doi:10.1016/j.mayocp.2019.01.013
6. Ma W, Zeng J, Montoya DJ, et al. Labyrinthin expression is associated with poor prognosis in patients with non-small-cell lung cancer. *Cancers*. 2023;15(3):924. doi:10.3390/cancers15030924
7. Wang CC, Shen WJ, Anuraga G, et al. Penetrating exploration of prognostic correlations of the FKBP gene family with lung adenocarcinoma. *J Pers Med*. 2022;13(1):49. doi:10.3390/jpm13010049
8. Han B, Zheng R, Zeng H, et al. Cancer incidence and mortality in China, 2022. *J Natl Cancer Cent*. 2024;4(1):47–53. doi:10.1016/j.jncc.2024.01.006
9. Wu J, Zhou Z, Li J, et al. CHD4 promotes acquired chemoresistance and tumor progression by activating the MEK/ERK axis. *Drug Resist Updat*. 2023;66:100913. doi:10.1016/j.drup.2022.100913
10. Shi J, Yang Y, Chen F, et al. RPL36A activates ERK pathway and promotes colorectal cancer growth. *Transl Oncol*. 2025;51:102170. doi:10.1016/j.tranon.2024.102170
11. Pal N, Banerjee K, Sarkar S, Mandal TK, Bhabak KP. Synthesis of thiazolidinedione- and triazole-linked organoselenocyanates and evaluation of anticancer activities against breast cancer with mechanistic investigations. *Chemistry*. 2025;31(11):e202403026. doi:10.1002/chem.202403026
12. Popova NV, Jücker M. The role of mTOR signaling as a therapeutic target in cancer. *Int J Mol Sci*. 2021;22(4):1743. doi:10.3390/ijms22041743
13. Xing JN, Shang YN, Yu ZL, Zhou SH, Chen WY, Wang LH. LncRNA HCP5-encoded protein contributes to Adriamycin resistance through ERK/mTOR pathway-mediated autophagy in breast cancer cells. *Genes Dis*. 2024;11(4):101024. doi:10.1016/j.gendis.2023.06.002
14. Ge Y, Xiao B, Zhao R, et al. CARMIL1 regulates liver cancer cell proliferation by activating the ERK/mTOR pathway through the TRIM27/p53 axis. *Int Immunopharmacol*. 2024;134:112139. doi:10.1016/j.intimp.2024.112139
15. Gao Y, Wang Y, Wang X, et al. FABP4 regulates cell proliferation, stemness, apoptosis, and glycolysis in colorectal cancer via modulating ROS/ERK/mTOR pathway. *Discov Med*. 2023;35(176):361–371. doi:10.24976/Discov.Med.202335176.37
16. Paknia E, Chari A, Stark H, Fischer U. The ribosome cooperates with the assembly chaperone pICln to initiate formation of snRNPs. *Cell Rep*. 2016;16(12):3103–3112. doi:10.1016/j.celrep.2016.08.047
17. Wahl MC, Will CL, Lührmann R. The spliceosome: design principles of a dynamic RNP machine. *Cell*. 2009;136(4):701–718. doi:10.1016/j.cell.2009.02.009
18. Staley JP, Guthrie C. An RNA switch at the 5′ splice site requires ATP and the DEAD box protein Prp28p. *Mol Cell*. 1999;3(1):55–64. doi:10.1016/s1097-2765(00)80174-4
19. Fica SM, Mefford MA, Piccirilli JA, Staley JP. Evidence for a group II intron-like catalytic triplex in the spliceosome. *Nat Struct Mol Biol*. 2014;21(5):464–471. doi:10.1038/nsmb.2815
20. Toor N, Keating KS, Taylor SD, Pyle AM. Crystal structure of a self-spliced group II intron. *Science*. 2008;320(5872):77–82. doi:10.1126/science.1153803
21. Li D, Zhang X, Zhang Y, et al. Development and validation of a nomogram model for predicting residue of partially cystic thyroid nodules after ultrasound-guided ethanol and thermal ablation. *Front Endocrinol*. 2023;14:1128248. doi:10.3389/fendo.2023.1128248
22. Valles I, Pajares MJ, Segura V, et al. Identification of novel deregulated RNA metabolism-related genes in non-small cell lung cancer. *PLoS One*. 2012;7(8):e42086. doi:10.1371/journal.pone.0042086
23. Quidville V, Alsafadi S, Goubar A, et al. Targeting the deregulated spliceosome core machinery in cancer cells triggers mTOR blockade and autophagy. *Cancer Res*. 2013;73(7):2247–2258. doi:10.1158/0008-5472.CAN-12-2501
24. Peters S, Adjei AA, Gridelli C, et al. Metastatic non-small-cell lung cancer (NSCLC): ESMO clinical practice guidelines for diagnosis, treatment and follow-up. *Ann Oncol*. 2012;23(Suppl 7):vii56–64. doi:10.1093/annonc/mds226
25. Xuhong JC, Qi XW, Zhang Y, Jiang J. Mechanism, safety and efficacy of three tyrosine kinase inhibitors lapatinib, neratinib and pyrotinib in HER2-positive breast cancer. *Am J Cancer Res*. 2019;9(10):2103–2119.
26. Aust S, Schwameis R, Gagic T, et al. Precision medicine tumor boards: clinical applicability of personalized treatment concepts in ovarian cancer. *Cancers*. 2020;12(3):548. doi:10.3390/cancers12030548
27. Lu L, Cao Z, Wang A, Chen L, Sun J, Li Z. Pathological complete response to neoadjuvant lorlatinib in a patient with stage IIIA ALK-positive non-small cell lung cancer: a case report. *Transl Lung Cancer Res*. 2024;13(7):1742–1748. doi:10.21037/tlcr-24-112

28. Zhu L, Zhang X, Sun Z. SNRPB promotes cervical cancer progression through repressing p53 expression. *Biomed Pharmacother*. 2020;125:109948. doi:10.1016/j.biopha.2020.109948
29. Liu N, Wu Z, Chen A, et al. SNRPB promotes the tumorigenic potential of NSCLC in part by regulating RAB26. *Cell Death Dis*. 2019;10(9):667. doi:10.1038/s41419-019-1929-y
30. Correa BR, de Araujo PR, Qiao M, et al. Functional genomics analyses of RNA-binding proteins reveal the splicing regulator SNRPB as an oncogenic candidate in glioblastoma. *Genome Biol*. 2016;17(1):125. doi:10.1186/s13059-016-0990-4
31. Eini M, Parsi S, Barati M, et al. Bioinformatic investigation of micro RNA-802 target genes, protein networks, and its potential prognostic value in breast cancer. *Avicenna J Med Biotechnol*. 2022;14(2):154–164. doi:10.18502/ajmb.v14i2.8882
32. Wu Q, Liao R, Miao C, et al. Oncofetal SNRPE promotes HCC tumorigenesis by regulating the FGFR4 expression through alternative splicing. *Br J Cancer*. 2024;131(1):77–89. doi:10.1038/s41416-024-02689-5
33. Wang H, Yang C, Li D, Wang R, Li Y, Lv L. Bioinformatics analysis and experimental validation of a novel autophagy-related signature relevant to immune infiltration for recurrence prediction after curative hepatectomy. *Aging*. 2023;15(7):2610–2630. doi:10.18632/aging.204632
34. Li FP, Liu GH, Zhang XQ, et al. Overexpressed SNRPB/D1/D3/E/F/G correlate with poor survival and immune infiltration in hepatocellular carcinoma. *Am J Transl Res*. 2022;14(6):4207–4228.
35. Chari A, Golas MM, Klingenhäger M, et al. An assembly chaperone collaborates with the SMN complex to generate spliceosomal SnRNPs. *Cell*. 2008;135(3):497–509. doi:10.1016/j.cell.2008.09.020
36. Ouyang D, Yang P, Cai J, Sun S, Wang Z. Comprehensive analysis of prognostic alternative splicing signature in cervical cancer. *Cancer Cell Int*. 2020;20:221. doi:10.1186/s12935-020-01299-4
37. Zhan YT, Li L, Zeng TT, Zhou NN, Guan XY, Li Y. SNRPB-mediated RNA splicing drives tumor cell proliferation and stemness in hepatocellular carcinoma. *Aging*. 2020;13(1):537–554. doi:10.18632/aging.202164
38. Peng N, Li J, He J, et al. c-myc-mediated SNRPB upregulation functions as an oncogene in hepatocellular carcinoma. *Cell Biol Int*. 2020;44(5):1103–1111. doi:10.1002/cbin.11307
39. Anchi T, Tamura K, Furihata M, et al. SNRPE is involved in cell proliferation and progression of high-grade prostate cancer through the regulation of androgen receptor expression. *Oncol Lett*. 2012;3(2):264–268. doi:10.3892/ol.2011.505
40. Bakheet T, Al-Mutairi N, Doubi M, Al-Ahmadi W, Alhosaini K, Al-Zoghaibi F. A computational recognition analysis of promising prognostic biomarkers in breast, colon and lung cancer patients. *Int J Mol Sci*. 2025;26(3):1017. doi:10.3390/ijms26031017
41. Tapak L, Saidijam M, Sadeghifar M, Poorolajal J, Mahjub H. Competing risks data analysis with high-dimensional covariates: an application in bladder cancer. *Genomics Proteomics Bioinf*. 2015;13(3):169–176. doi:10.1016/j.gpb.2015.04.001
42. Lv J, He Y, Li L, Wang Z. Alternative splicing events and splicing factors are prognostic in adrenocortical carcinoma. *Front Genet*. 2020;11:918. doi:10.3389/fgene.2020.00918
43. Bauer MA, Ashby C, Wardell C, et al. Differential RNA splicing as a potentially important driver mechanism in multiple myeloma. *Haematologica*. 2021;106(3):736–745. doi:10.3324/haematol.2019.235424
44. Stefanovska B, Vicier CE, Dayris T, et al. Rapalog-mediated repression of tribbles pseudokinase 3 regulates pre-mRNA splicing. *Cancer Res*. 2020;80(11):2190–2203. doi:10.1158/0008-5472.CAN-19-2366
45. Li Z, Pützer BM. Spliceosomal protein E regulates neoplastic cell growth by modulating expression of cyclin E/CDK2 and G2/M checkpoint proteins. *J Cell Mol Med*. 2008;12(6A):2427–2438. doi:10.1111/j.1582-4934.2008.00244.x
46. Xu J, Kong L, Oliver BA, et al. Constitutively active autophagy in macrophages dampens inflammation through metabolic and post-transcriptional regulation of cytokine production. *Cell Rep*. 2023;42(7):112708. doi:10.1016/j.celrep.2023.112708
47. Chen X, Sun Y, Wang B, Wang H. Prognostic significance of autophagy-related genes Beclin1 and LC3 in ovarian cancer: a meta-analysis. *J Int Med Res*. 2020;48(11):300060520968299. doi:10.1177/0300060520968299
48. Cao Z, Tian K, Ran Y, et al. Beclin-1: a therapeutic target at the intersection of autophagy, immunotherapy, and cancer treatment. *Front Immunol*. 2024;15:1506426. doi:10.3389/fimmu.2024.1506426
49. Li X, Yang KB, Chen W, et al. CUL3 (cullin 3)-mediated ubiquitination and degradation of BECN1 (beclin 1) inhibit autophagy and promote tumor progression. *Autophagy*. 2021;17(12):4323–4340. doi:10.1080/15548627.2021.1912270
50. Jovanović L, Nikolić A, Dragičević S, Jović M, Janković R. Prognostic relevance of autophagy-related markers p62, LC3, and Beclin1 in ovarian cancer. *Croat Med J*. 2022;63(5):453–460. doi:10.3325/cmj.2022.63.453
51. Scervino MVM, Fortes MAS, Vitzel KF, et al. Autophagy signaling in hypertrophied muscles of diabetic and control rats. *FEBS Open Bio*. 2023;13(9):1709–1722. doi:10.1002/2211-5463.13677
52. Loh JS, Rahim NA, Tor YS, Foo JB. Simultaneous proteasome and autophagy inhibition synergistically enhances cytotoxicity of doxorubicin in breast cancer cells. *Cell Biochem Funct*. 2022;40(4):403–416. doi:10.1002/cbf.3704
53. Zhu J, Cai Y, Xu K, et al. Beclin1 overexpression suppresses tumor cell proliferation and survival via an autophagy-dependent pathway in human synovial sarcoma cells. *Oncol Rep*. 2018;40(4):1927–1936. doi:10.3892/or.2018.6599